

Experimental Demonstration of “Cold” Low Contact Resistivity Ohmic Contacts on Moderately Doped n-Ge with in-situ Atomic Hydrogen Clean

Ashish Agrawal¹, Jeongwon Park², Dheeraj Mohata¹, Khaled Ahmed² and Suman Datta¹

¹Department of Electrical Engineering, The Pennsylvania State University, University Park, PA 16802, USA

²Applied Materials, Inc., 3050 Bowers Ave., Santa Clara, CA 95054, USA

Abstract—Low contact resistivity ohmic contacts are demonstrated on *n*-Ge at doping level N_D of $1 \times 10^{19} \text{ cm}^{-3}$. Atomic Hydrogen (H^*) clean was shown to reduce the specific contact resistivity (ρ_C) by 7% for the first time, due to reduction of barrier height of 70meV compared to the unclean sample. Improvement was primarily due to the reduction of the germanium oxide, GeO_x , and surface passivation at the interface by H atoms as confirmed by energy-dispersive X-ray spectroscopy (EDS). The ρ_C of $2.7 \times 10^{-5} \Omega\text{-cm}^2$, at a moderate doping density of $1 \times 10^{19} \text{ cm}^{-3}$, is the lowest with the minimum possible thermal budget.

Introduction—A metal-oxide-semiconductor field effect transistor (MOSFET) with Ge as the channel material has received much attention, mainly because the electron and hole mobilities are $2 \times$ and $4 \times$ higher than those in Si, respectively. Key challenges faced by Ge for *n*-MOSFET is the Fermi level pinning near the valence band which prevents formation of low contact resistivity ohmic contact, thereby degrading ON-current. Further, n-type dopants diffuse readily in Ge, limiting the thermal budget for formation of ohmic contact. In this work, we demonstrate formation of “cold” ohmic contact to n-Ge and study the effect of in-situ atomic H^* clean on ρ_C for moderately doped *n*-Ge. Finally, we benchmark it with existing experimental and modeled results.

Results and Discussion—Fig. 1(a) shows the schematic of a 10^{19} cm^{-3} doped *n*-Ge structure grown on *p*-Si as substrate with *i*-Ge as a metamorphic buffer layer to accommodate the dislocations due to lattice mismatch. In-situ atomic H^* clean was performed before PVD TiN deposition for one sample, in addition to an unclean, control sample of TiN/*n*-Ge. Fig. 1(b) shows the simulated energy band diagram indicating high Schottky barrier height of 0.57 eV [1] from conduction band edge due to pinned Fermi level. In order to extract the experimental ρ_C of deposited TiN on *n*-Ge, self-isolating circular TLM (CTLM) structures were fabricated on the unclean and H^* dry cleaned samples. I-V data was measured for increasing TLM contact spacing (Fig. 2a); both samples showed symmetric, linear, non-rectifying characteristics for the entire current range, indicating ohmic contact formation between TiN and *n*-Ge. The total resistance extracted from I-V results as a function of contact spacing for both samples is shown in Fig. 2b. By numerically fitting the experimental resistance based on the CTLM model, ρ_C was extracted for both the samples. Low ρ_C of $2.9 \times 10^{-5} \Omega\text{-cm}^2$, a sheet resistivity of $45 \Omega/\square$ and $L_T=8\mu\text{m}$ was obtained for unclean sample. An improvement of 7% was observed on H^* cleaned sample exhibiting ρ_C of $2.7 \times 10^{-5} \text{ ohm-cm}^2$. Cross-section TEM showed the presence of an interlayer at the TiN/*n*-Ge interface for the unclean sample, which was absent for the atomic H^* cleaned interface. Energy Dispersive Spectroscopy (EDS) performed at the interface indicated monolayer oxide at the interface for unclean sample (Fig.4a); a clear reduction in the O peak was observed with atomic H^* clean (Fig4b). In order to understand the dominant conduction mechanism across the contact, measurements at high temperature upto 150°C were performed on both the samples. As shown in Fig. 5, reduction in ρ_C was observed for $T=25^\circ\text{C}$ to 150°C for both samples. Modeling indicated thermionic field emission (TFE) as the dominant conduction mechanism for transport across TiN/*n*-Ge for $N_d=10^{19} /\text{cm}^3$. To assess the observed improvement in contact resistivity with other data in the literature, we have benchmarked our experimental results (Fig. 6). Additionally, ρ_C as a function of N_D was modeled for Ge for comparison considering thermionic emission, thermionic field emission and field emission conduction mechanisms depending on the doping range. We have obtained the lowest contact resistivity for a non-alloyed, un-annealed M-S contact on *n*-Ge for $N_D=10^{19} \text{ cm}^{-3}$, which is 4 orders of magnitude lower than a similar M-S structure reported for similar doping [1]. The calculated ρ_C for the given N_D is $4 \times$ higher than that obtained experimentally, indicating a reduced Schottky barrier height of 0.5eV. In-situ H^* clean results in removal of O from the surface and passivates with H^* before metal deposition as confirmed by EDS, alleviating Fermi pinning [2]. If similar surface condition is maintained, very low ρ_C of $2 \times 10^{-9} \Omega\text{-cm}^2$ can be obtained for high $N_D=10^{20} \text{ cm}^{-3}$ using this process. Experimentation with higher doped *n*-Ge is in progress. The low contact resistivity achieved using minimal thermal budget is of much significance in order to prevent S/D dopant diffusion during high temperature contact annealing processes (Fig. 7), increasing the junction depth and in turn, degrading short channel effects for scaled *n*-Ge MOSFETs. Table I summarizes the experimental ρ_C data along with dopant and thermal treatment to elucidate the low thermal budget advantage of this process.

Conclusion—We demonstrate the lowest specific contact resistivity of $2.7 \times 10^{-5} \Omega\text{-cm}^2$ for a non-alloyed, un-annealed M-S contact on *n*-Ge for low doping $N_D=10^{19} \text{ cm}^{-3}$ with in-situ atomic H^* dry clean and PVD TiN deposition. Fermi pinning was reduced by surface passivation by H^* treatment resulting in decrease in SBH. Low thermal budget processing allows this process to be well-suited for ultra-scaled quantum well FET applications preventing diffusion of dopants in source/drain or channel material into the barriers.

[1] K. Martens et. al. *Appl. Phys. Lett.* 98, 2011

[2] J. Cho et. al. *Phys. Rev. B*, 46, 1992

[3] S. Raghunathan et. al. *ECS Transactions*, 33, 2010

[4] G. Thareja et. al. *IEDM* 2010

[5] K. Martens et. al. *IEDM* 2010.

[6] J. Oh et. al. *Proc. of ICSSDM*, 2010

[7] M. Iyota et. al. *Appl. Phys. Lett.* 98, 2011.

[8] C. O. Chui et. al. *Appl. Phys. Lett.* 83, 2003

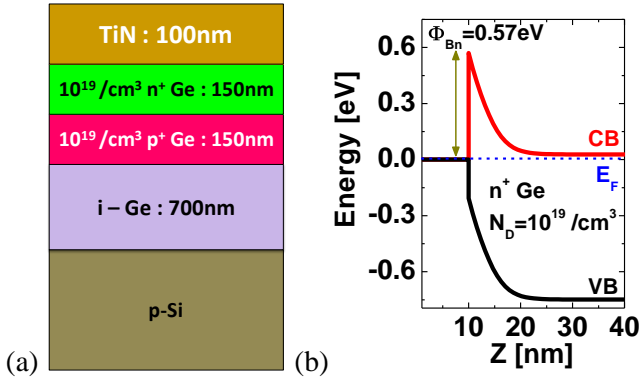


Fig. 1 (a) Schematic of the TiN/n-Ge layer structure grown on p-Si (b) Calculated energy band diagram for TiN/n-Ge for $N_d=10^{19}/\text{cm}^3$ indicating pinned Schottky barrier height of 0.57eV.

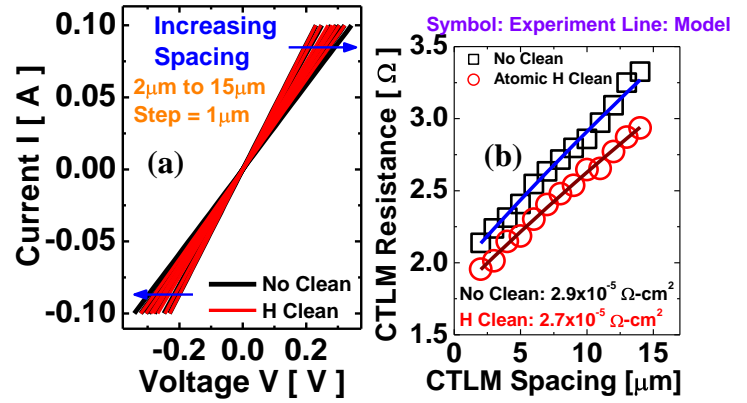


Fig. 2 (a) Experimental I-V characteristics of unclean and in-situ H cleaned samples for increasing slit width (b) Extracted total resistance as a function of CTLM spacing for unclean and atomic H cleaned samples, indicating reduced contact resistivity for latter case.

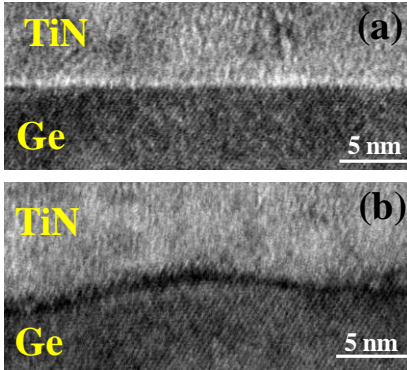


Fig. 3 Cross-section TEM of (a) unclean TiN/n-Ge sample showing thin interlayer at the interface, (b) atomic H* cleaned sample showing no interlayer at the TiN/n-Ge interface

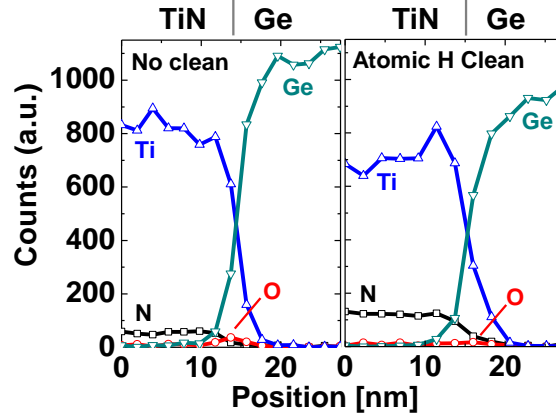


Fig. 4 Energy Dispersive Spectra (EDS) of unclean and atomic H cleaned sample at the interface. Oxygen peak is observed at the interface of unclean sample, which was reduced as a result of atomic H* clean, resulting in improved contact resistivity for latter sample.

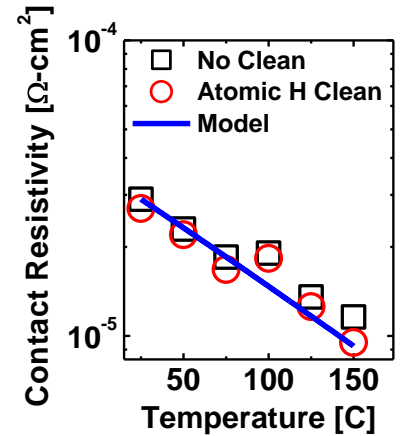


Fig. 5 Experimental and modeled contact resistivity characteristics at $T=25^\circ\text{C}$ to 150°C for unclean and atomic H cleaned samples.

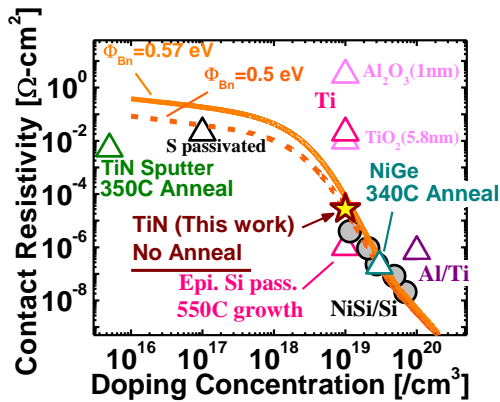


Fig. 6 Benchmarking of experimental contact resistivity as a function of doping concentration for various contact architectures on n-Ge, along with analytical model for SBH=0.57eV and 0.5eV. Measured contact resistivity on n-Ge is similar to NiSi/n-Si for same doping.

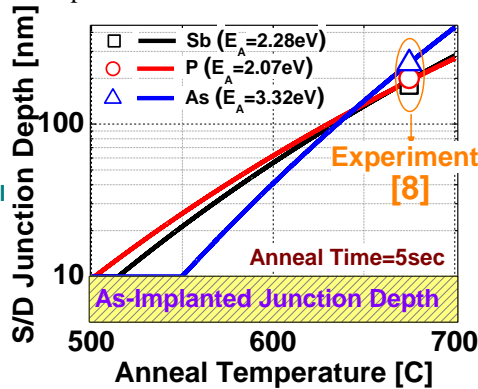


Fig. 7 Simulated source/drain junction depth vs. contact anneal temperature for common n-type dopants P, As and Sb on Ge with indicated activation energy. As implanted junction depth was assumed to be 10nm and anneal time was set as 5sec. Minimal thermal budget prevents dopant diffusion leading to better short-channel effects for scaled n-Ge MOSFETs

Contact	Dopant	Doping (/cm ³)	Anneal. (C)	ρ_c (Ω-cm ²)	
Ti	P	N.A.	650	6×10^{-5}	[3]
Ti	Sb	10^{20}	LSA	7×10^{-7}	[4]
NiGe	As	10^{19}	250/300	2.5×10^{-6}	[5]
NiGe	N.A.	N.A.	300	4×10^{-5}	[6]
TiN	N.A.	6×10^{15}	340	4×10^{-3}	[7]
TiN	P	10^{19}	No Anneal	2.7×10^{-5}	--

Table I Contact resistivity values on n-Ge reported till date for various contact architectures indicating doping and annealing conditions.